ENGINEERING TRANSACTIONS • *Engng. Trans.* • **44**, 2, 229–251, 1996
Polish Academy of Sciences • Institute of Fundamental Technological Research

ULTIMATE LOAD AND POSTFAILURE BEHAVIOUR OF BOX-SECTION BEAMS UNDER PURE BENDING

M. KOTEŁKO (ŁÓDŹ)

In this work the load-carrying capacity and plastic collapse mechanisms of thin-walled, rectangular and trapezoidal box-section beams subject to pure bending are investigated. The postbuckling elastic analysis is carried out using the effective width approach while the plastic buckling load is evaluated using the total strain theory. The failure of the beam is assumed to be initiated by buckling in a flange so that the flange mechanism of failure is expected. The analysis of plastic collapse mechanisms is carried out using basic assumptions of the rigid-plastic theory. The true (kinematically permissible) plastic mechanisms are taken into consideration. Three different theoretical solutions concerning the plastic moment capacity at a yield line are taken into account. Corresponding formulae for plastic moment at yield lines situated both in flanges and webs of the thin-walled beam are evaluated. The energy method is used in order to evaluate the bending moment capacity in terms of rotation angle of a global plastic hinge. The total energy of plastic deformation absorbed during rotation of the global plastic hinge is formulated and the bending moment is derived from this formula. For both rectangular and trapezoidal cross-section beams the idealized geometry of a global plastic hinge is based on the results of experimental tests. In the case of elastic buckling, the ultimate bending moment is determined approximately at the intersection point of two curves representing the bending moment in terms of the rotation angle: the postbuckling curve based upon approximate nonlinear analysis and the post-failure curve derived from the collapse mechanism analysis. Bending moment - rotation angle diagrams based on numerical results of the theoretical analysis, are compared with graphs recorded during experimental four-point tests.

1. INTRODUCTION

Four separate phases are observed in the behaviour of a thin-walled beam in the complete range of loading, from zero up to and beyond the ultimate load (Fig. 1). The first phase is the pre-buckling one. The second phase is the nonlinear, post-buckling behaviour. Assuming that the buckling load of a particular plate member of the beam is less than that corresponding to the yield stress which is regarded to be equal to the limit of proportionality, after exceeding the buckling load, the local buckling and also the interaction of different buckling modes occurs. Since deflections of plate members are relatively large and, simultaneously, constitutive relations between stresses

and strains are still linear, the second phase can be regarded as an elastic, post-buckling behaviour. The third phase is initiated by the first yield in one of the plate members and is the elasto-plastic one, in which both geometrical and physical relations are nonlinear. At the highest point of this phase, the bending moment is at its ultimate value and, at the same instant, the last, post-failure phase begins. The propagation of yield regions proceeds and, in consequence, the plastic mechanism of failure is created.

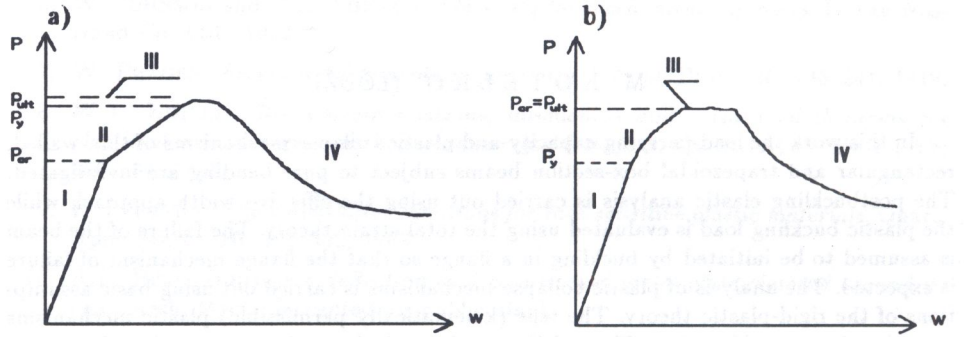

FIG. 1. Exemplary load-deflection graphs of the thin-walled structure; a) elastic buckling, b) plastic buckling.

Also four phases can be observed in the beam's behaviour, when the plastic buckling occurs: the pre-buckling elastic phase, the elasto-plastic one, the buckling plateau and the post-failure phase.

The post-buckling, elastic behaviour of thin-walled beams considered as plate assemblies has been analysed by many authors, starting from von Kármán fundamental publications [1]. Analytical solutions as well as numerical procedures concerning the post-buckling behaviour of thin-walled girders were published in [2, 3]. The interaction of different buckling modes was analysed in [3, 5]. An interactive buckling analysis was also carried out by KOITER and PIGNATARO [4] who investigated a nonlinear, post-buckling path of thin-walled structure (beam, column) using the second order approximation based on the linear analysis. This approach enables us to determine approximately a load-carrying capacity on the basis of a simplified threshold criterion. The method was further developed by KOŁAKOWSKI [17] and can be classified as a *lower bound* solution. The effective width approach was applied by RHODES [6] in order to analyze the post-buckling behaviour of plates.

The elasto-plastic behaviour of plates under compression was analysed in [2]. There are very few publications concerning the thin-walled columns as plate assemblies [7] in the elasto-plastic range. Since the theoretical analysis of the problem is extremely complicated, efficient analytical solutions of the

elasto-plastic post-buckling behaviour of thin-walled beams have not been found in practice. The plastic buckling of separate plates was analysed by VOLMIR [1] and very comprehensively discussed in [2].

The post-ultimate collapse behaviour of thin-walled box-section beams was analysed in [8, 9]. Both authors applied the rigid-plastic theory in order to describe the kinematically permissible plastic mechanisms of failure. The same approach was presented in [10] where plastic collapse mechanisms in thin-walled beams of triangular cross-section were described.

The principal aim of the present work is the approximate evaluation of the load-carrying capacity of a thin-walled beam by means of combined results of nonlinear, post-buckling analysis with the analysis of plastic mechanism of failure. This approach leads to an *upper bound* estimation of the load-carrying capacity. The method enables us not only to solve the ultimate load problem but to answer the question of postfailure behaviour of the structure as well. The second information is particularly desirable if a designer wants to know whether the collapse of the structure happens rapidly or proceeds slowly with warnings preceding the catastrophe. From the other point of view, the presented approach allows us to avoid the extremely complicated analysis of the elasto-plastic range of loading.

An evaluation of the plastic moment capacity at yield lines situated not only in beam members subject to compression but also to in-plane bending, when different theoretical models of stress distribution in the yield line cross-section are taken into account, was the second problem to be solved since no effective solution of the problem has been known so far. The solution obtained within the present work leads to a higher level of collapse curve approximation which is of great importance as far as the *upper bound* estimation of load-carrying capacity, carried out by means of method mentioned above, is concerned. The comparative analysis of different theoretical models of collapse mechanisms of thin-walled, box section beams is an additional aim of the paper.

2. THE SUBJECT AND BASIC ASSUMPTIONS OF THE ANALYSIS

The subject of investigation was the thin-walled, rectangular and trapezoidal box-section beam under pure bending (Fig. 2). The beam cross-section was a rectangle or an isosceles trapezoid. The bending moment was acting in the plane created by the axis of the cross-section symmetry and the longitudinal axis of the beam.

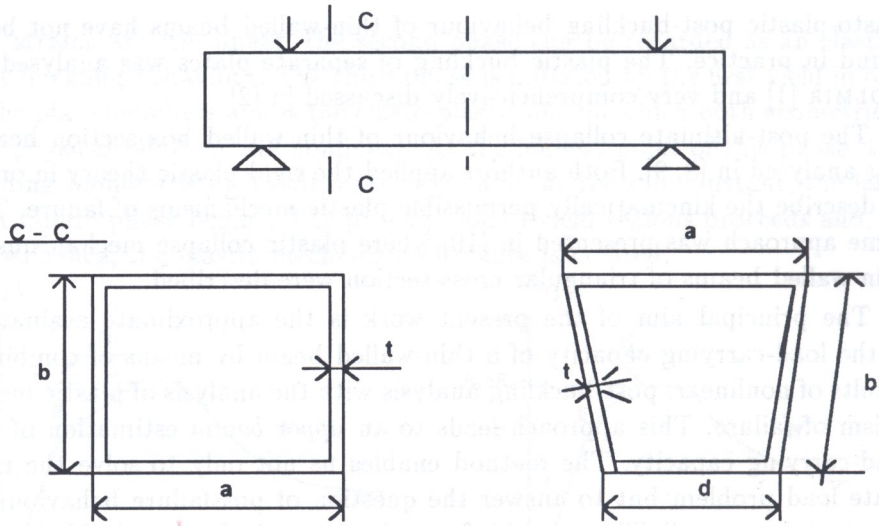

FIG. 2. Thin-walled beam under pure bending.

The analysis was carried out on the basic assumptions which were as follows:

- the failure of the beam was initiated by buckling of the flange subject to compression and also the first yield was assumed to occur in the compressed flange or, in a particular case, in the flange in tension (see Sec. 3.1), so that the *flange mechanism* was expected,
- kinematically permissible (true mechanisms) were taken into account only, i.e. plastic mechanisms were assumed to be well developed and membrane strains in walls of the global plastic hinge were neglected [11],
- plastic zones were concentrated and could be regarded either as stationary or travelling yield-lines of the global plastic hinge [8, 10],
- wall continuity was assumed in two main sections: in the cross-section of the global plastic hinge and in the axial, longitudinal section of the beam,
- the rigid-perfectly plastic behaviour was assumed for beam's material as far as the plastic mechanism analysis was concerned.

3. Approximate analysis of the post-buckling behaviour

3.1. Elastic buckling

The post-buckling, elastic behaviour of the beam (when the buckling load is less than that corresponding to the yield stress) was analysed using the effective width approach. The buckling stress of the flange in compression as

well as its effective width in terms of actual, post-buckling stress was determined using approximate formulae proposed by RHODES [6]. The buckling stress was evaluated using the following expression:

$$\sigma_{cr} = k\pi^2 D/a^2 t, \tag{3.1}$$

where

$$k = 7 - [1.8(b/a)/(0.15 + b/a)] - 0.091(b/a)^3, \qquad D = Et^3/12.$$

The effective width was determined as follows:

$$a_e = a[1 + 14(\sqrt{\sigma_y/\sigma_{cr}} - 0.35)^4]^{-0.2}. \tag{3.2}$$

The corresponding formulae concerning the effective cross-section (centroid and second moment of area) are given in Appendix A.

Since the effective width decreases due to the increase of the actual bending moment and subsequently – to the increase of the compressive stress in the flange, the second moment of area is a function of the increasing load. In order to calculate the rotation angle in terms of the bending moment capacity of the beam, the following numerical procedure was applied.

The ratio

$$n = \sigma/\sigma_{cr}$$

(where σ was the actual average stress in the flange under compression) was calculated for a certain value of the bending moment, while one of two possible equations was used with regard to one of the following possibilities:

CASE 1 (first yield occurs on the side in compression)

$$M - n\sigma_{cr}\frac{I_{ze}}{z_{max}} = 0, \tag{3.3}_1$$

CASE 2 (first yield occurs on the side in tension)

$$M - F_2(n, \sigma_{cr}) = 0. \tag{3.3}_2$$

Relation describing $F_2(n, \sigma_{cr})$ is given in Appendix A.

Knowing the ratio n it is possible to take the second step of the procedure – calculation of the actual effective width and second moment of area. Subsequently, the rotation angle and deflection of the beam may be evaluated using simple formulae derived from the beam theory.

3.2. *Plastic buckling*

The post-buckling plastic behaviour of a beam of relatively compact cross-section was analysed on the assumption mentioned in Sec. 2, i.e. buckling and the first yield were expected in the flange under compression.

A theory of plastic buckling of plates based on the total strain theory was developed by VOLMIR [1]. The plastic buckling stress of a simply supported rectangular plate, derived by Volmir, is as follows:

$$\sigma_{cr} = k'\pi^2 D/a^2 t, \tag{3.4}$$

where

$$k' = 0.25[13(1-r)+3s],$$
$$r = f_1(E_c/E), \qquad s = f_2(E_t/E).$$

Coefficients r and s depending on secant (E_s) and tangent (E_t) moduli may be evaluated from a stress-strain diagram of the plate material. Since beam's flange under compression buckles in the plastic range, the beam cannot carry any additional bending moment. Thus the ultimate bending moment is obtained as follows:

$$M_{ult} = \sigma_{cr}\frac{I_z}{z_{max}}. \tag{3.5}$$

4. THE COLLAPSE MECHANISM ANALYSIS

4.1. *Plastic mechanisms of failure*

A survey of different theoretical models of true collapse mechanisms in thin-walled beams is given in this paragraph. The first theoretical model of the true plastic mechanism in the thin-walled beam of rectangular cross-section was evaluated by KECMAN [8].

The geometry of Kecman's mechanism is shown in Fig. 3 and denoted by R1. The mechanism applicable to beams with a relatively high width-to-depth ratio (b/a), typically for values above 2, was evaluated by KRÓLAK and KOTEŁKO [16]. It is also shown in Fig. 3 and denoted by R3. A quasi-mechanism observed during tests [13, 14] carried out on long, both rectangular and trapezoidal cross-section beams (of relatively thick walls) was presented in [14]. In this paper a simplification of this model (a true mechanism) has been evaluated. It is shown as R2 in Fig. 3. It may be regarded as a transition between the Kecman's mechanism R1 and the mechanism R3. Details concerning the geometry of this mechanism are given in Appendix B.

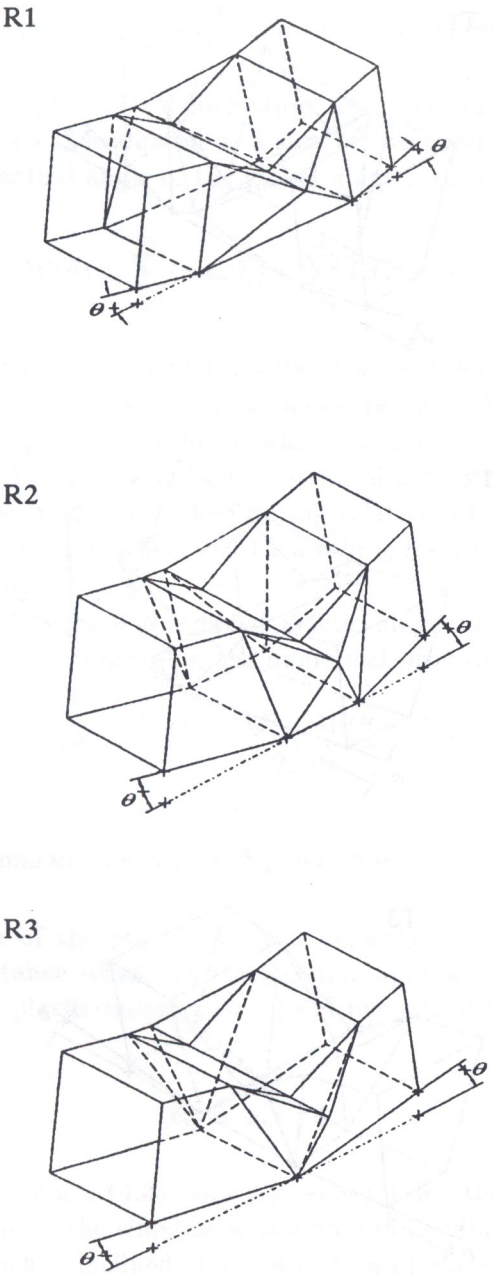

FIG. 3. True plastic mechanisms in a beam of rectangular cross-section.

KRÓLAK and KOTEŁKO [16] considered the bending collapse mechanisms in trapezoidal cross-section beams. Three different mechanisms according to different b/a ratios were evaluated (Fig. 4). The first one was the Kecman

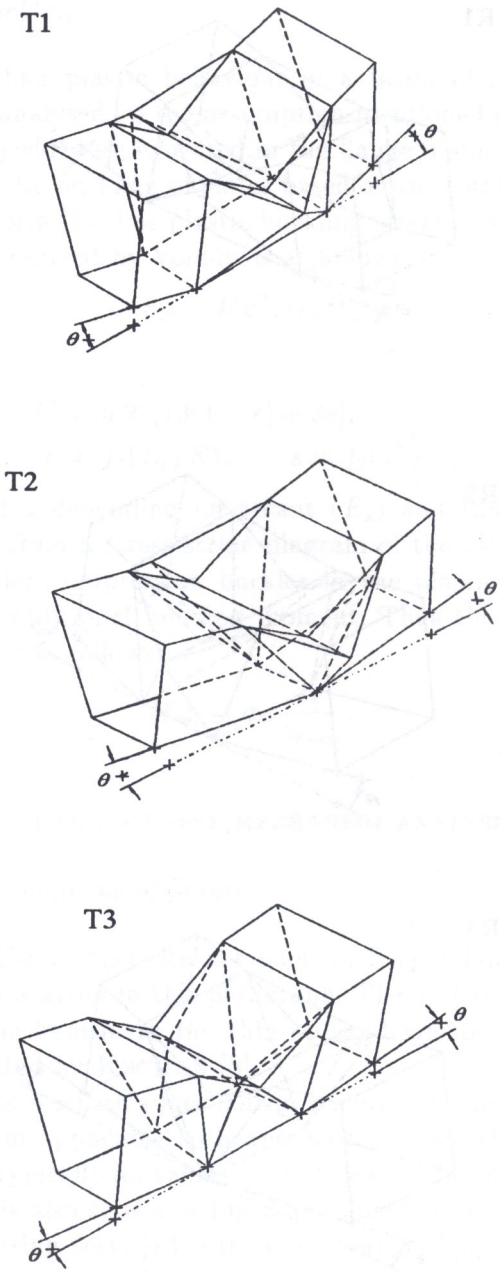

FIG. 4. True plastic mechanisms in a beam of trapezoidal cross-section.

mechanism (T1), two others were found in cross-sections of a relatively high b/a ratio ($b/a > 1.5$). The mechanism T3 was considered to be theoretically possible for beams with relatively closely spaced diaphragms.

The analysis of the collapse behaviour was carried out using the energy method [8, 10].

The total energy of plastic deformation, absorbed during rotation of the global plastic hinge was evaluated as a sum of two components, in terms of the angle Θ – an actual angle of the global hinge rotation:

$$W(\theta) = \sum_{i=1}^{n}(md_i\beta_i) + \sum_{i=1}^{2} F_i(m, r, \theta), \tag{4.1}$$

where m was the plastic moment capacity at a yield line.

The first component was a sum of the energy absorbed during relative rotation by angle $\beta_i(\Theta)$ of two hinge walls along a stationary yield line of the length $d_i(\Theta)$. F_1 and F_2 are components of the deformation energy of local plastic hinges [8], 10] absorbed during relative rotation of hinge walls along travelling yield lines, where $r(\Theta)$ is a *rolling radius* of a travelling yield line [8].

The bending moment of the global plastic hinge was derived from the total energy of deformation, using the numerical procedure:

$$M(\theta) = \frac{W(\theta + \Delta\theta) - W(\theta - \Delta\theta)}{2\Delta\theta}. \tag{4.2}$$

4.2. Plastic moment capacity at the yield line

The evaluation of the plastic moment capacity m at a yield line is of substantial importance when the mechanisms approach is applied. In the papers [8–10] the plastic moment at a yield line was determined as a fully plastic moment:

$$m_p = \sigma_y t^2/4. \tag{4.3}$$

However, the formula (4.3) does not account for the reduction of the plastic moment due to the simultaneous action of bending and compression on a yield line which is inclined to the direction of normal stresses induced by the bending moment and compression load. The problem of a separate plate under compressive load was widely discussed by ZHAO and HANCOCK [15] and also mentioned by SIN [9]. In Fig. 5 three theoretical models of the stress distribution at the yield line, quoted by ZHAO and HANCOCK [15] and also SIN [9], are presented.

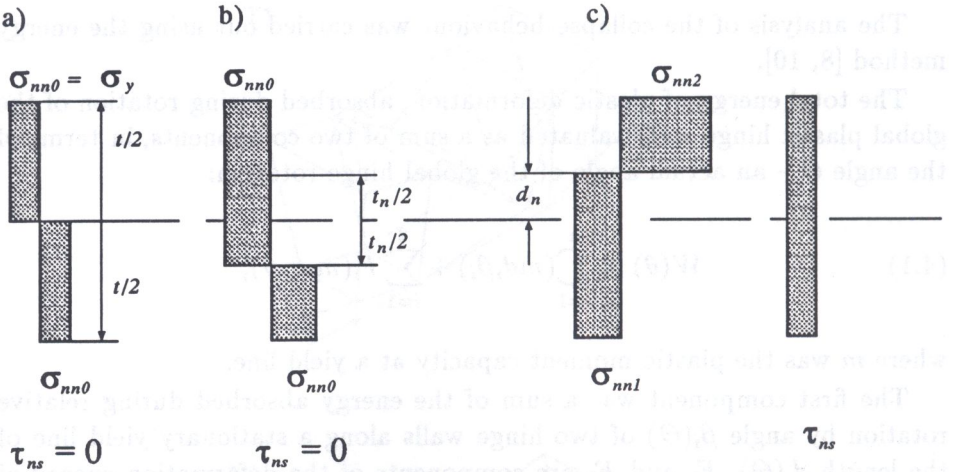

FIG. 5. Stress distribution at the yield line; a) fully plastic moment, b) Mouty, c) Murray (1984) and Sin (1985).

4.2.1. Plastic moment at a yield line in a plate member under compression. The plastic moment capacity at a yield line in the compressed plate (Fig. 6) may be evaluated in the following way:

$$m = m_p P_i(\sigma/\sigma_y, \gamma), \tag{4.4}$$

where P_i is a function depending on the theoretical model applied, σ is a compression stress acting on the boundary of the plate (Fig. 6), and σ_y is the yield stress.

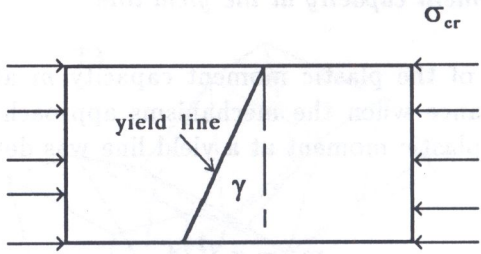

FIG. 6. Plate under uniformly distributed compressional stress.

According to three theoretical models shown in Fig. 5, functions P_i are as follows:

- fully plastic moment:

$$P_1 = 1, \tag{4.5}_1$$

- Mouty's model [15]:

$$P_2 = 1 - (\sigma/\sigma_y)^2 \cos^4 \gamma, \tag{4.5}_2$$

• Sin's model [9]:

$$(4.5)_3 \qquad P_3 = \frac{1-(\sigma/\sigma_y)^2}{\sqrt{1-0.75(\sigma/\sigma_y)^2\sin^2\gamma[\sin^2\gamma+4(1-\sin^2\gamma)]}}.$$

Formulae $(4.5)_2$ and $(4.5)_3$ are based upon the Huber and von Mises yield criterion.

4.2.2. Plastic moment at a yield line in a plate member subject to in-plane bending. The same problem concerning a plate as a member of a more complex section (box-section beam) has not been evaluated so far. Consequently the approach presented above could not be applied to the beam as a whole. The problem was elaborated in the present paper and a proposal of an effective solution is given below. The flanges are considered to be subjected to uniformly distributed stresses of magnitude equal to the buckling stress, thus a compression stress σ is assumed to be equal to the buckling stress ($\sigma = \sigma_{cr}$). The plastic moment at a yield line situated in a flange is expressed as follows:

$$(4.6) \qquad m_f = m_p P_i(\sigma_{cr}/\sigma_y, \gamma),$$

where P_i are given by formulae (4.5) at the assumption of $\sigma = \sigma_{cr}$.

The web is assumed to be an assembly of strips of unit width which are subjected to either compressive or tensile stresses of various magnitudes, depending on its location relative to the neutral axis of bending (Fig. 7).

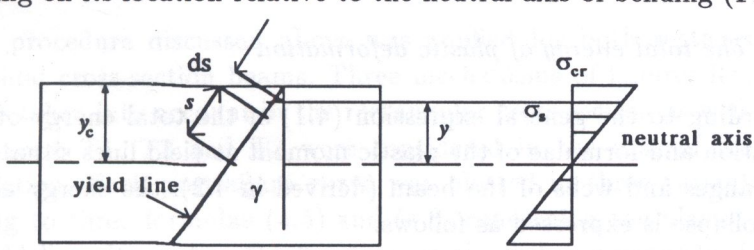

FIG. 7. Plate subjected to in-plane bending.

The magnitude of the plastic moment at an inclined yield line in a strip located at a distance y from the neutral axis, as shown in Fig. 7, is given by

$$(4.7) \qquad m_{wy} = m_p P_i(\sigma_s/\sigma_y, \gamma),$$

where

$$\sigma_s = \sigma_{cr}\frac{y}{y_c}.$$

After integrating with respect to s and, subsequently, to y,

$$m_w = m_p \int P_i(\sigma_s/\sigma_y, \gamma)\, ds,$$

the following relation was obtained:

$$m_w = m_p \Omega_i(\sigma_{cr}/\sigma_y, \gamma), \tag{4.8}$$

where Ω_i is a function depending on the theoretical model applied and on the shape of the cross-section. For the rectangular box-section, functions Ω_i are as follows, according to the formulae (4.5) applied:

- fully plastic moment

$$\Omega_1 = 1, \tag{4.9}_1$$

- formula based on Mouty's stress distribution

$$\Omega_2 = 1 - (1/3)(\sigma_{cr}/\sigma_y)^2 \cos^4\gamma, \tag{4.9}_2$$

- formula based on Murray and Sin's stress distribution

$$\Omega_3 = \frac{\alpha_1 - \alpha_2}{\alpha_{no}} \left[(C_\gamma)^{-1} - (C_\gamma^2)^{-3/2}\right], \tag{4.9}_3$$

where

$$\begin{aligned} \alpha_1 &= \arcsin(C_\gamma \alpha_{no}/2), \\ \alpha_2 &= \arcsin(-C_\gamma \alpha_{no}/2), \\ C_\gamma &= \sqrt{3}\sin(\gamma\sqrt{\sin^2\gamma + 4(1 - \sin^2\gamma)}, \\ \alpha_{no} &= \sigma_{cr}/\sigma_y. \end{aligned}$$

4.3. The total energy of plastic deformation

According to the general expression (4.1) of the total energy of plastic deformation and formulae of the plastic moment at yield lines situated both in the flanges and webs of the beam (derived in 4.2), the energy absorbed at the collapse is expressed as follows:

$$W(\theta) = \sum_{j=1}^{m} m_{fj} d_j \beta_j + \sum_{k=1}^{n} m_{wk} d_k \beta_k + \sum_{i=1}^{2} F_i(m_{wi}, r, \theta), \tag{4.10}$$

where m_{fj} – plastic moment at a yield line situated in a flange, m_{wk}, m_{wi} – plastic moment at a yield line situated in a web, m – number of stationary yield lines in the flanges, n – number of stationary yield lines in the webs.

The expression given above is a general one for all mechanisms described in Sec. 4.1. Details concerning the total energy of plastic deformation for plastic mechanism R2 (evaluated in this paper) are given in Appendix B.

5. The load-carrying capacity

As far as the elastic buckling of the flange in compression is concerned, the ultimate bending moment capacity of the beam was evaluated approximately by combining the solution based upon the effective width approach (Sec. 3.1) with the results of plastic mechanism analysis (Sec. 4.1). Thus the ultimate bending moment was determined at the intersection of two curves representing the bending moment in terms of the rotation angle of the beam at the middle of the span: the post-buckling curve plotted using the numerical procedure based on formulae (3.1)–(3.3) and the postfailure curve derived from equations (4.1)–(4.10). Coordinates of the intersection point were determined by the iterative bisection procedure.

In the case of the plastic buckling of the flange under compressive stress, the formula (3.5) was applied in order to evaluate the ultimate bending moment capacity.

The bending moment capacity in terms of the rotation angle at the middle of the span was plotted in the whole range of loading from zero up to and beyond the ultimate bending moment. The pre-buckling state was evaluated using the beam theory, while the elastic, post-buckling curve or the plastic buckling plateau was derived using the procedures mentioned in Sec. 3.1 or 3.2, respectively.

6. Discussion of the results

The procedure discussed above was applied for both rectangular and trapezoidal cross-section beams. Three mechanisms of failure: R1, R2 and R3 were taken into account in the rectangular cross-section as well as three mechanisms: T1, T2 and T3 were considered in the case of trapezoidal cross-section. Each postfailure curve was plotted in three variants, corresponding to three formulae (4.5) and (4.8) concerning the plastic moment at a yield line situated in the flange or in the web, respectively. Diagrams plotted on the basis of numerical results of the theoretical analysis were compared with numerically processed load-deflection graphs recorded during experimental, four-point tests carried out on rectangular cross-section beams of relatively slender walls [12], as well as on both the rectangular and trapezoidal, compact cross-section beams (relatively thick walls) [14].

In Fig. 8 and 9 diagrams concerning rectangular cross-section beams of relatively slender walls are presented. In Fig. 8 theoretical curves of mechanisms R1, R2, and R3 respectively, calculated from the fully plastic moment

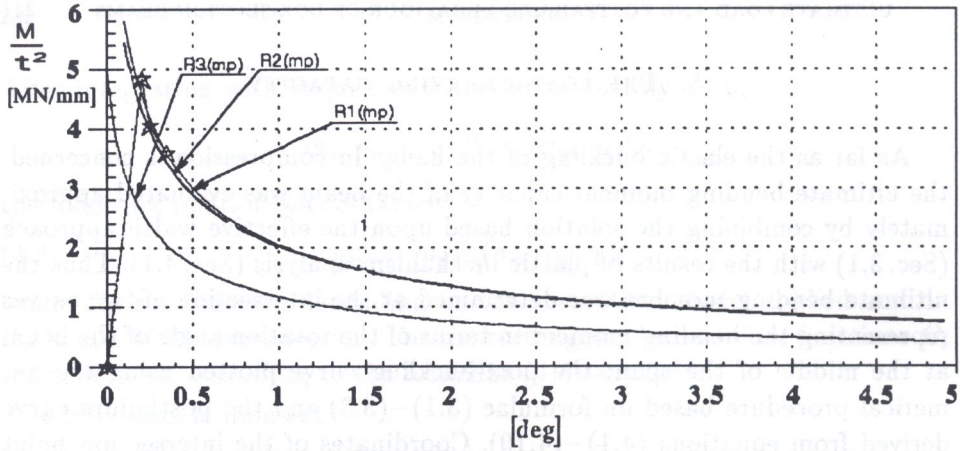

FIG. 8. Rectangular box-section beam of slender walls; $a = 110\,\text{mm}$, $b = 140\,\text{mm}$, $\sigma_y = 250\,\text{MPa}$. Comparison of different models of plastic mechanisms with the results of experiments.

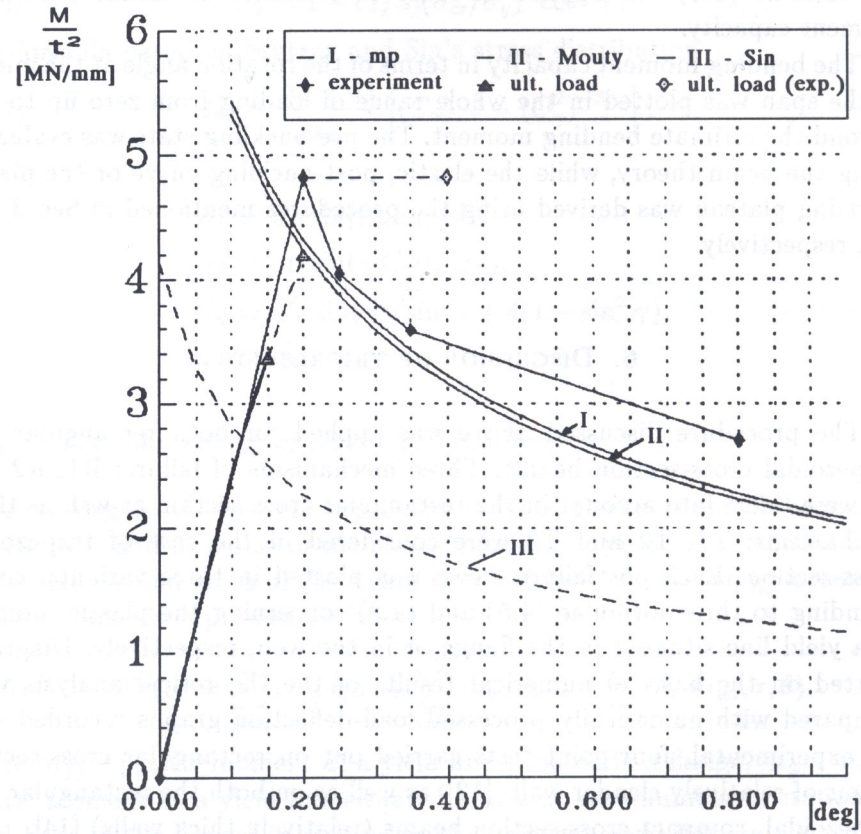

FIG. 9. Rectangular box-section beam of slender walls (data as in Fig. 8). Elastic buckling. Comparison of different models of plastic moment capacity at a yield-line with experimental results.

equation (4.8) at a yield line are presented. The asterisks indicate results of experiments. On the basis of the diagram shown it can be said that the mechanism R1 (Kecman's) is the most adequate model of all those reviewed, although the curves R1 and R2 are very close to each other when this particular, rectangular cross-section beam is considered.

In Fig. 9 the theoretical pre- and post-buckling paths are presented as well as three curves of the mechanisms R1 corresponding to three different formulae of the plastic moment capacity at a yield line. Theoretical results are compared with the results of experiment. The theoretical and experimental values of the ultimate bending moment are indicated.

In Fig. 10 theoretical curves of mechanisms R1, R2 and R3 are compared with the results of experiments carried out on rectangular, compact cross-section beams [14]. Both in this case and in the case of the beam of relatively slender walls the most adequate model proved to be the first one (R1).

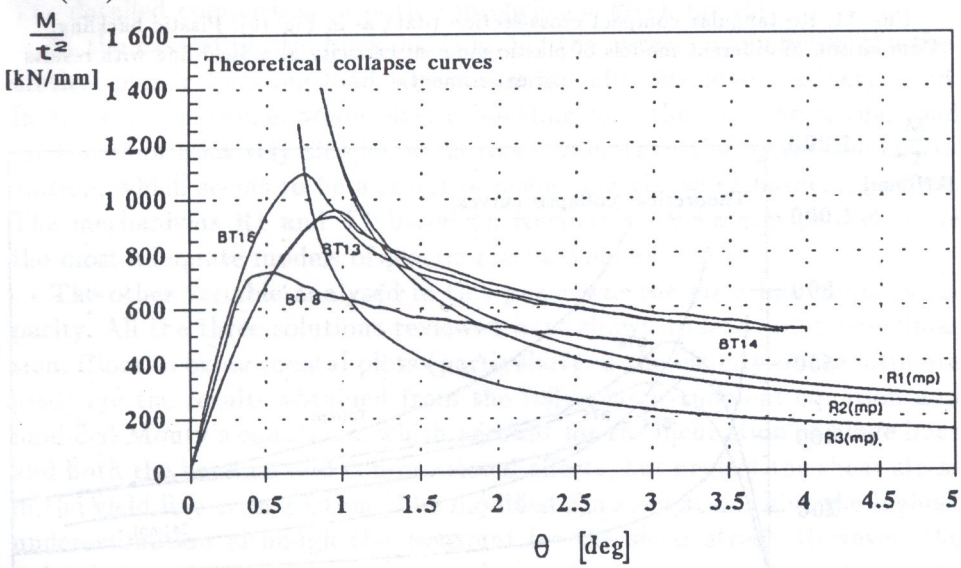

FIG. 10. Rectangular compact cross-section; $a = 50\,\text{mm}$, $b = 60\,\text{mm}$, $\sigma_y = 168\,\text{MPa}$. Comparison of different models of plastic mechanisms with results of experiments.

Figure 11 presents the same experimental results compared with the theoretical, prebuckling path and plastic buckling plateau, as well as theoretical curves of the mechanism R1 calculated by means of three different formulae for the plastic moment capacity at a yield line.

In Fig. 12 diagrams for trapezoidal, compact cross-section beam are presented. Theoretical curves of mechanisms T1, T2 and T3 (fully plastic moment at a yield line) are compared with experimental plots [14]. The curve

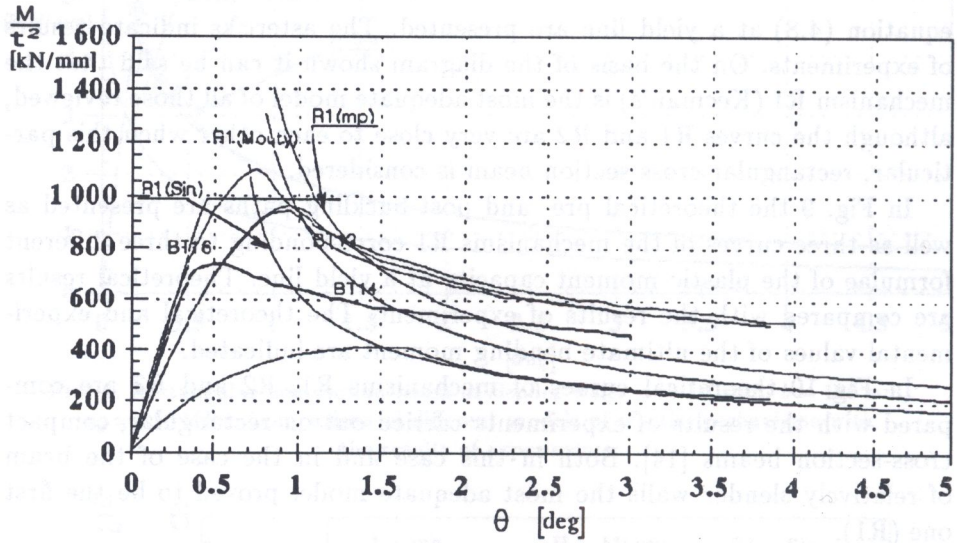

FIG. 11. Rectangular compact cross-section (data as in Fig. 10). Plastic buckling. Comparison of different models of plastic moment capacity at a yield-line with results of experiment.

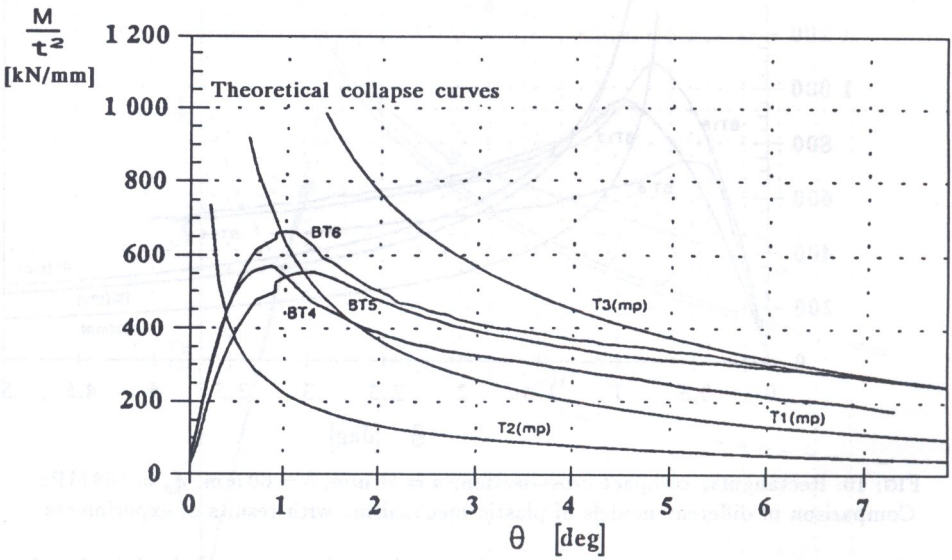

FIG. 12. Trapezoidal compact cross-section; $a = 60\,\text{mm}$, $b = 40\,\text{mm}$, $d = 35\,\text{mm}$, $\sigma_y = 168\,\text{MPa}$. Comparison of different models of plastic mechanisms with results of experiments.

T1 happens to lie the closest to the results of experiment. The plastic mechanism T3 was mentioned only in passing since this purely hypothetical model was never observed during experimental investigation.

7. Final conclusions

A good agreement of theoretical and experimental values of ultimate load obtained for beams of relatively slender walls (Fig. 9) has been obtained in the case of elastic buckling. It confirms that the combination of the approximate, nonlinear post-buckling analysis and the analysis of plastic mechanisms of failure can be applied in order to evaluate the load-carrying capacity of the structure. It has to be underlined that since the energy approach was adopted to analyse true plastic mechanisms, the approximate, theoretical value of the ultimate bending moment can be classified as an *upper bound* solution. In the other extreme, an alternative *lower bound* approach which enables us to determine effectively the load-carrying capacity of a structure, is that developed in [17]. Both approximations – presented in this paper and in references mentioned above – allow to avoid an extremely complicated analysis of the elasto-plastic behaviour of a structure. The detailed comparison of both approaches is given in [18].

In the case of plastic buckling (Fig. 11) the agreement between the theoretical plastic buckling load with an actual ultimate load was very good. In the other extreme, when elastic buckling was the case, an actual load for beams of relatively slender walls was higher than the *upper bound* estimation, which seems to be a result of neglecting the work-hardening effect. The mechanisms R1 and T1 based on Kecman's mechanism proved to be the most adequate models of plastic mechanisms of failure.

The other variable analysed in this paper was the yield line moment capacity. All the three solutions reviewed have shown to lead to underestimation. Close to experimental plots (particularly in the vicinity of the ultimate load) are the results obtained from the fully plastic moment equation and modified Mouty's equations, which account for the inclination of hinge lines and both the bending and compressional effects, but neglect the shear stress in the yield line cross-section. The modified Sin's equations give the highest underestimation although they account for the shear stress. However, the point to be underlined here is that the mechanism approach used neglects all work hardening and membrane strain effects which both tend to raise the bending moment capacity.

When examining the diagrams it can be noted that the bending moment capacity of the collapsing beams in the experiments were not reduced as rapidly as predicted by the theoretical models at the final stage of failure. In the other extreme, in the vicinity of the ultimate load the agreement of theoretical and experimental post-failure curves is much better (Fig. 9). This again shows that the work hardening effect is of significant importance in the final phase of mechanism development.

Finally, it should be said that true mechanisms (assumed for all models in this study) which are relatively simple to analyse, can be regarded as a good approximation of actual mechanism of failure, but to obtain a solution of high accuracy, a quasi-mechanism which incorporates regions of membrane strains should be used. Strain hardening effects are also recommended to be taken into consideration.

Appendix A. Effective cross-section calculation

A. Yielding in the boundary fibre in compression

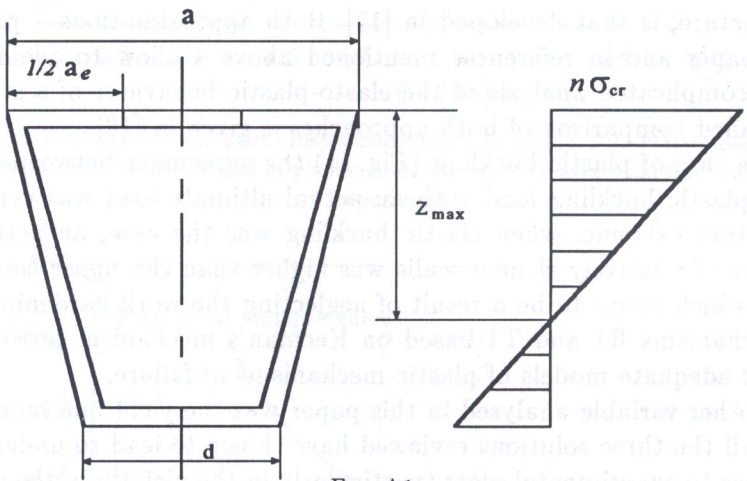

Fig. A1.

Position of neutral axis of effective cross-section:

$$z_{\max} = \frac{b \sin\alpha(b+d)}{a_e + 2b + d}.$$

Effective second moment of area:

$$I_{ze} = a_e t z_{\max}^2 + (1/6)b^3 t \sin^2\alpha + 2bt(0.5b\sin\alpha - z_{\max})^2 + dt(b\sin\alpha - z_{\max})^2.$$

B. Yielding in the boundary fibre in tension

Neutral axis position:

$$f = \frac{n\sigma_{cr}\sin\alpha(b-b_y)}{\sigma_y + n\sigma_{cr}}.$$

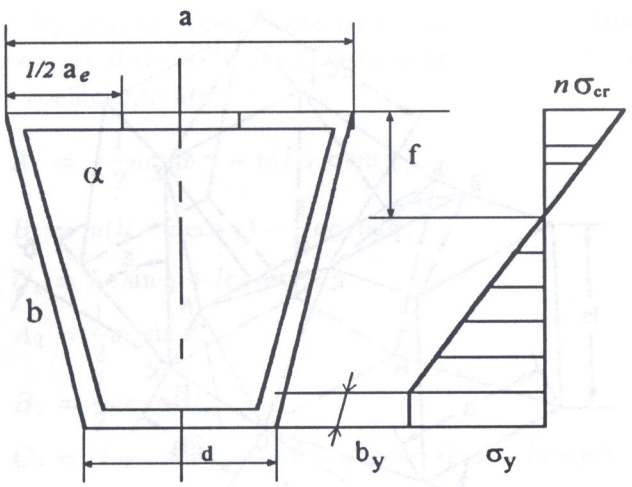

FIG. A2.

Width of the yield strip in tension:

$$b_y = \frac{n\sigma_{cr}(a_e + b) - \sigma_y(d + b)}{\sigma_y + n\sigma_{cr}}.$$

Function $F_2(n, \sigma_{cr})$ – see Eq. $(3.3)_2$:

$$F_2(n, \sigma_{cr}) = t\Big[(f^2/3\sin\alpha)n\sigma_{cr} + \sigma_y[(b - b_y)\sin\alpha - f]\left[\frac{1}{3}\left(b - b_y - \frac{f}{\sin\alpha}\right) + (2b_y + d)\right]\Big].$$

APPENDIX B. PLASTIC MECHANISM R2

All quantities describing the geometry of the mechanism shown in Fig. B1 were expressed in terms of the rotation angle θ of the global plastic hinge except for two independent parameters c and h which were evaluated on the basis of experimental observations [14]. Thus, basic quantities characterising the geometry of the mechanism are as follows:

$$\gamma = \cos^{-1}\left[\frac{h}{c} + \frac{R}{c}\cos(\theta + \varepsilon)\right], \qquad R = \sqrt{b^2 + (c - h)^2},$$

where

$$\varepsilon = \operatorname{arctg}\left[\frac{b}{c - h}\right], \qquad u = \frac{b^2 - l^2}{2b}$$

and

$$l = R\sin(\theta + \varepsilon) - c\sin\gamma, \qquad \xi = \operatorname{arctg}(u/l).$$

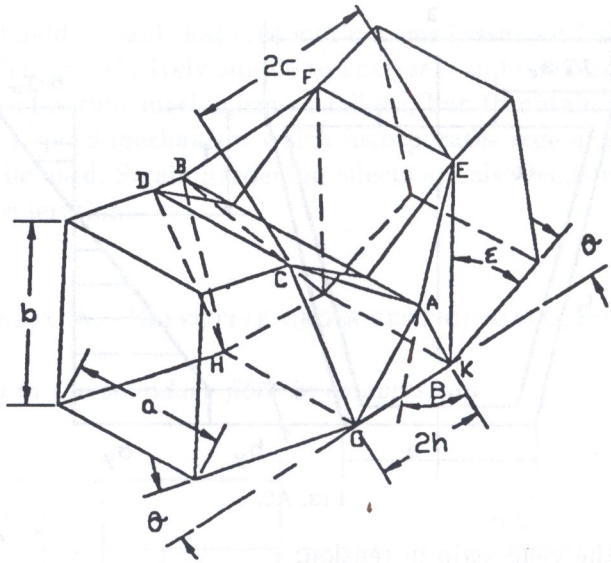

FIG. B1. Mechanism R2.

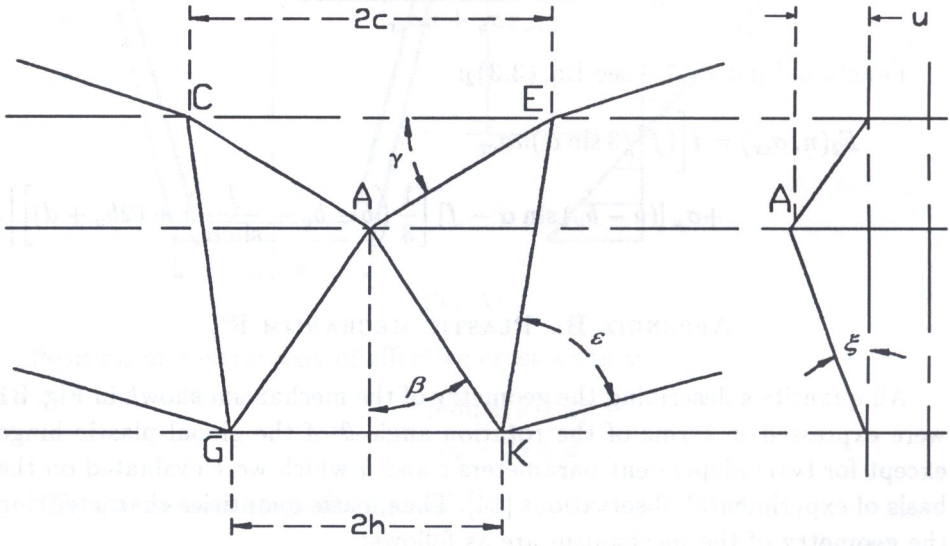

FIG. B2. Mechanism R2 – front and side view.

The rotation angle η of the wall ACG and the undeformed part of the web is expressed as follows:

$$\cos\eta = \pm\frac{A_1A_2 + B_1B_2 + C_1C_2}{\sqrt{A_1^2 + B_1^2 + C_1^2}\sqrt{A_2^2 + B_2^2 + C_2^2}},$$

where A_1, A_2, B_1, B_2, C_1 and C_2 are coefficients of two planes ACG and the undeformed part of the web, determined in three-dimensional coordinate system. These coefficients are:

$$A_1 = -\frac{1}{2}ac\sin\gamma - u(l + c\sin\gamma),$$

$$B_1 = u(h - c\cos\gamma) - \frac{1}{2}ac\cos\gamma,$$

$$C_1 = hc\sin\gamma + lc\cos\gamma,$$

$$A_2 = \frac{1}{2}ac\sin\theta,$$

$$B_2 = \frac{1}{2}ac\cos\theta,$$

$$C_2 = (l + c\sin\gamma)c\cos\theta - c^2\cos\gamma\sin\theta - hc\sin\theta.$$

According to the general formula (4.10) given in Sec. 4.3, the components of the energy of plastic deformation are expressed in terms of angle θ and are as follows:

$$W_1 = \sum_{j=1}^{m} m_{fj}d_j\beta_j = W_{AB} + W_{CD+...} + W_{GH+...} + W_{GK+...} + W_{CE+...}$$

$$= m_{f1}(a + 2u)2\gamma + m_{f2}2a(\gamma - \theta) + m_{f3}2a\theta + m_{f4}4h\xi + m_{f5}2c\pi,$$

$$W_2 = \sum_{j=1}^{m} m_{wk}d_k\beta_k = W_{.CG+...} = m_w^{(1)}4R(\pi - \eta);$$

$$W_3 = F_1(m_w, r, \theta) = W_{AG+...} = \frac{8}{3}m_w^{(2)}\frac{uw}{r}$$

is the energy absorbed during rotation of two walls of the global plastic hinge along the travelling yield lines AG and AK;

$$W_4 = F_2(m_w, r, \theta) = W_{AC+...} = 4\frac{m_w^{(3)}cu}{r}$$

is the energy absorbed at the local plastic hinges A and B,
where

$$r = c\left(0.07 - \frac{\theta}{35}\right)$$

is the rolling radius [8], and

$$w = \sqrt{(b - u)^2 + h^2}.$$

The total energy of plastic deformation is a sum of four components given above:

$$W(\theta) = W_1 + W_2 + W_3 + W_4.$$

ACKNOWLEDGMENTS

The study was supported by the grant KBN No PB 0923/p4/930.

REFERENCES

1. A.S. VOLMIR, *Stability of deformable media* [in Russian], Nauka, Moskva 1967.
2. *Post-buckling and load carrying capacity of thin-walled girders of flat walls* [in Polish], M. KRÓLAK [Ed.], PWN, Warszawa-Łódź 1990.
3. M. KRÓLAK and Z. KOŁAKOWSKI, *Stability and post-buckling of thin-walled, box-section girders subject to bending and compression (tension)* [in Polish], Arch. Bud. Maszyn, **28**, 2, 1981.
4. W.T. KOITER and M. PIGNATARO, *A general theory for the interaction between local and overall buckling of stiffened panels*, Delft University, WTHD Report No 556, 1976.
5. Z. KOŁAKOWSKI, *Interactive buckling of thin-walled, elastic structures* [in Polish], Zesz. Nauk. Politech. Łódzkiej, No 653, Łódź 1992.
6. J. RHODES, *Effective widths in plate buckling; contribution to: Developments in thin-walled structure-1*, J. RHODES and A.C. WALKER [Eds.], Applied Science Publishers, London 1981.
7. R. GRĄDZKI and K. KOWAL-MICHALSKA, *Post-buckling behaviour of orthotropic compressed columns in elastic and elasto-plastic range* [in Polish], Proc. of VIIth Symposium of Stability of Structures, Bielsko-Biała 1994.
8. D. KECMAN, *Bending collapse of rectangular and square section tubes*, Int. J. Mech. Sci., **25**, 9-10, 1983.
9. K.W. SIN, *The collapse behaviour of thin-walled sections*, Ph.D. Thesis, Dept. of Mech. Engng., Univ. of Strathclyde, Glasgow UK 1985.
10. M. KOTEŁKO and M. KRÓLAK, *Collapse behaviour of triangular cross-section girders subject to pure bending*, Thin-Walled Struct., **15**, 2, Elsevier Appl. Sci., 1993.
11. N.W. MURRAY, *Introduction to the theory of thin-walled structures*, Clarendon Press, Oxford 1986.
12. M. KOTEŁKO, *Comparative theoretical and experimental analysis of collapse mechanisms in box-section girders* [in Polish], Proc. of VIIth Symposium of Stability of Structures, Bielsko-Biała 1994.
13. M. KOTEŁKO and VYNX T.H. LIM, *The large deflection behaviour of thin-walled trapezoidal cross-section beams under pure bending* [in Polish], Proc. of VIIth Conf. "Developments in Heavy Duty Machines Design", Zakopane 1994.
14. M. KOTEŁKO, J. RHODES and VYNX T.H. LIM, *Post-failure behaviour of box-section beams under pure bending (an experimental study)* [accepted to be published in Thin-Walled Struct., Elsevier Appl. Sci.].
15. X.L. ZHAO and G.J. HANCOCK, *A theoretical analysis of the plastic moment capacity of an inclined yield line under axial force*, Thin-Walled Struct., **15**, 3, Elsevier Appl. Sci., 1993.

16. M. KOTEŁKO and M. KRÓLAK, *An approximate method of load-carrying capacity evaluation in thin-walled beams subject to bending* [in Polish], Proc. of VIth Conf. "Heavy Duty Machines – Developments in Design, Operating and Investigation", Zakopane 1993.

17. Z. KOŁAKOWSKI, *Influence of modification of boundary conditions on load-carrying capacity in thin-walled columns in the second order approximation*, Int. J. Solids and Struct., **30**, 19, 1993.

18. M. KOTEŁKO and Z. KOŁAKOWSKI, *Post-buckling and collapse behaviour of thin-walled beam-columns*, Proc. of Int. Conf. on Lightweight Struct. in Civil Engng. (LSCE'95), Warszawa 1995.

DEPARTMENT OF STRENGTH OF MATERIALS AND STRUCTURES
ŁÓDŹ UNIVERSITY OF TECHNOLOGY, ŁÓDŹ.

Received December 8, 1995.